HHS Public Access

Author manuscript

Am J Surg Pathol. Author manuscript; available in PMC 2021 April 23.

Published in final edited form as:

Am J Surg Pathol. 2018 August ; 42(8): 1010–1026. doi:10.1097/PAS.0000000000001086.

Bronchiolar Adenoma: Expansion of the Concept of Ciliated Muconodular Papillary Tumors with Proposal for Revised Terminology Based on Morphologic, Immunophenotypic and Genomic Analysis of 25 cases.

Jason C. Chang, MD[1], **Joseph Montecalvo, MD**[1], **Laetitia Borsu, PhD**[1], **Shaohua Lu, MD**[2], **Brandon T. Larsen, MD, PhD**[3], **W. Dean Wallace, MD**[4], **Wichit Sae-Ow, MD**[5], **Alexander C. Mackinnon, MD, PhD**[6], **Hyunjae R. Kim, PhD**[1,7], **Anita Bowman, Msc**[1], **Jennifer L. Sauter, MD**[1], **Maria E. Arcila, MD**[1], **Marc Ladanyi, MD**[1], **William D. Travis, MD**[1], **Natasha Rekhtman, MD, PhD**[1]

[1.]Department of Pathology, Memorial Sloan Kettering Cancer Center, New York, NY, USA.

[2.]Department of Pathology, Zhongshan Hospital, Fudan University, Shanghai, China.

[3.]Department of Laboratory Medicine and Pathology, Mayo Clinic, Phoenix, AZ, USA.

[4.]Department of Pathology, David Geffen School of Medicine, University of California Los Angeles, Los Angeles, CA, USA.

[5.]Department of Pathology, the Queen's Medical Center, Honolulu, HI, USA.

[6.]Department of Pathology, Medical College of Wisconsin, Milwaukee, WI, USA.

[7.]Texas Children's Cancer and Hematology Centers, Baylor College of Medicine, Houston, TX, USA.

Abstract

We have identified 25 lesions involving alveolar lung parenchyma characterized by nodular proliferation of bland bilayered bronchiolar-type epithelium containing a continuous layer of basal cells. These lesions shared some histologic features with the recently described entity of ciliated muconodular papillary tumor (CMPT); however, the majority did not fit all diagnostic criteria in that they exhibited only focal or absent papillary architecture, and they had variable number of ciliated and mucinous cells, with some lesions entirely lacking one or both of these components. The morphologic and immunohistochemical features ranged from those resembling proximal bronchioles (proximal-type: moderate to abundant mucinous and ciliated cells; negative or weak TTF1 in luminal cells; n=8) to those resembling respiratory bronchioles (distal-type: scant or absent mucinous and ciliated cells; positive TTF1 in luminal cells; n=17). The hallmark of all lesions was a continuous layer of basal cells (p40 and CK5/6-positive). We provisionally designated these lesions as bronchiolar adenomas and analyzed their clinicopathologic and

Corresponding Author: Natasha Rekhtman, MD, PhD, Department of Pathology, Memorial Sloan Kettering Cancer Center, 1275 York Avenue, New York, NY, 10065. rekhtman@mskcc.org.

Conflicts of Interest: The authors have disclosed that they have no significant relationship with, or financial interest in, any commercial companies pertaining to this article.

molecular features. All bronchiolar adenomas were discrete, sharply circumscribed lesions with a median size of 0.5 cm (range: 0.2 – 2.0 cm). Most lesions were either entirely flat (n=14) or contained focal papillary architecture (n=7); only 4 lesions, all proximal-type, were predominantly papillary, fitting the classic description of CMPT. Notably, of 9 lesions submitted for frozen section evaluation, 7 were diagnosed as adenocarcinoma. No post-surgical recurrences were observed for any lesions (median follow-up 11 months). Twenty-one bronchiolar adenomas underwent next-generation sequencing and/or immunohistochemistry for BRAF V600E, revealing mutation profiles similar to those previously described for CMPTs, including *BRAF* V600E mutations (n=8, 38%), unusual *EGFR* exon 19 deletions (n=2, 10%), *EGFR* exon 20 insertions (n=2, 10%), *KRAS* mutations (n=5, 24%), and *HRAS* mutations (n=1, 5%). The mutation profiles were similar in proximal- and distal-type lesions.

In conclusion, we describe a family of putatively benign clonal proliferations with a spectrum of morphology recapitulating various levels of the bronchiolar tree, of which only a minor subset fits the classic description of CMPT. Comparable mutation profiles and partially overlapping morphologic features across the spectrum of these lesions support their nosological relationship. We propose designating this entire family of lesions as bronchiolar adenomas, and that lesions currently designated CMPTs represent a subgroup of this family.

Keywords

Bronchiolar adenoma; ciliated muconodular papillary tumor; CMPT; bilayered; BRAF

INTRODUCTION

Adenomas of the lung recognized by the 2015 World Health Organization (WHO) classification include sclerosing pneumocytoma, alveolar adenoma, papillary adenoma, mucinous cystadenoma, and mucous gland adenoma.(1) Although the term bronchioloalveolar adenoma was sometimes used for what is now recognized as atypical adenomatous hyperplasia,(2) and the term bronchial adenoma was used in the past for carcinoid or salivary-type tumors,(3) the concept of an adenoma derived from bronchiolar epithelium is not well recognized. Considering adenomas that arise along the spectrum of lung airway epithelium from the proximal bronchus (mucous gland adenoma) to the peripheral alveolar structures (alveolar adenoma), we have identified a group of putatively benign lung neoplasms that appear to correspond to the anatomic epithelial cellular component of bronchioles. This led us to evaluate whether these tumors could be called bronchiolar adenoma based on morphologic, immunohistochemical, molecular and clinical findings.

Our study began by evaluating cases that appeared to fit the classical criteria for ciliated muconodular papillary tumor (CMPT). This is a relatively recently recognized entity that was first described by Ishikawa et al (4) in the Japanese literature in 2002. A handful of cases were subsequently reported in East Asian patients.(5–8) The entity remained largely unknown to pathologists outside of East Asia until a recent case series by Kamata and Yoshida et al,(9) who delineated the morphologic features of 10 CMPTs and subsequently described their molecular profiles.(10) Due to the increasing recognition of these tumors,

there has been an exploding number of case reports and small case series in recent years.(10–18) CMPT is currently thought to be a rare entity with a total number of 34 cases reported to date, with the vast majority of these cases still described in patients from East Asian countries.(4–18) The classic description of CMPT is a peripherally located nodular tumor with prominent papillary architecture consisting of tripartite cellular components of mucinous, ciliated, and basal cells.(4, 9) Despite the morphologic similarities to glandular papillomas, CMPTs grow entirely on alveolar walls with no association with the bronchial lumen. The molecular profile of CMPTs has been investigated in 20 cases to date.(7, 10, 13, 14, 16–18) The largest molecular series of CMPTs by Kamata et al (10) revealed the presence of peculiar driver mutations, most commonly *BRAF* V600E mutations or unusual *EGFR* exon 19 deletions, in 4 and 3 of 10 cases, respectively. Subsequent case reports and case series also described *AKT1* mutation, *KRAS* mutation, and *ALK* rearrangement in isolated cases.(14, 16–18) With the exception of *AKT1*, the other molecular alterations appeared mutually exclusive.

However, during the process of collecting lesions with features of CMPT, it became clear that the vast majority of cases did not have all of the classical histologic features. In all cases, these lesions were characterized by nodular proliferations of bland bronchiolar-type epithelium containing a continuous layer of basal cells, as described for classic CMPTs. However, unlike classic CMPTs, many lesions had only focal or absent papillary architecture, and they had variable numbers of ciliated and mucinous cells, with some lesions entirely lacking one or both of these components. We provisionally designated such lesions as bronchiolar adenomas (BA). Here we report on the clinicopathologic and molecular features of this group of lesions and summarize evidence supporting the proposal that these represent a family of adenomatous proliferations that encompasses but also substantially expands the concept of CMPT.

MATERIAL AND METHODS

Study design

Cases were identified prospectively between 2016 and 2017 and through retrospective search of Memorial Sloan Kettering Cancer Center (MSKCC) archive. Four cases were contributed by collaborators at UCLA Medical Center, Medical College of Wisconsin, Mayo Clinic Arizona, and Fudan University, China (one case each). The clinical and radiologic features were reviewed, and the histologic features were analyzed on the resection specimens. This study was approved by the institutional review board of MSKCC.

Immunohistochemistry

Immunohistochemical antibodies included p40 (Biocare; clone BC28, 1:200), TTF1 (Ventana; clone 8G7G3/1, prediluted), CK5/6 (Ventana; clone D5/16B4, prediluted), Napsin-A (Leica; clone IP64, 1:200), BRAF V600E (Spring Bio; clone VE1, 1:800), ALK (Cell Signaling; clone D5F3, prediluted), and CC10 (Santa Cruz; goat polyclonal IgG, 1:50). Immunohistochemistry was performed following standard procedures on either Ventana (Ventana Medical Systems, Tucson, AZ) or DAKO (DAKO USA, Santa Clara, CA) automated instruments. Immunohistochemical stains submitted from outside institutions

were reviewed. Due to the known labeling of normal cilia for BRAF V600E,(10) only cytoplasmic staining was regarded as positive.

Molecular analysis

Overall, 19 of 25 BAs underwent molecular analysis by next generation sequencing (NGS) or a multigene panel. Sixteen cases were analyzed by NGS at MSKCC, including 13 cases by a 98-gene Ampliseq Cancer Hotspot Panel (ThermoFisher Scientific, full list in Supplemental Table S1) and 3 cases by a 410-gene MSK-IMPACT (full list in Supplemental Table S2) panel. Three cases were analyzed outside of MSKCC using Ion Ampliseq Cancer Hotspot Panels (50 genes and 6 genes) and Amplification Refractory Mutation System (ARMS). Six of the 25 cases could not be tested due to insufficient or unavailable material.

For the cases processed at MSKCC, DNA extraction was performed using standard methods on formalin-fixed paraffin-embedded tissue on both tumor and matched normal tissue for 14 cases, while 2 additional cases were tested on tumor only, as normal tissue was unavailable. For Ampliseq samples, the amplicon library preparation was performed using 10 ng of FFPE DNA per reaction, as recommended by the manufacturer. In brief, the DNA was mixed with a primer pool containing all primers for generating the 3425 amplicons and with the Ion AmpliSeq HiFi master mix and was transferred to a PCR thermocycler (Eppendorf Mastercycler). The quality and quantity of the amplicon was assessed using the Agilent 2100 Bioanalyzer (Agilent technologies). Sequences were analyzed with the Torrent Variant Caller plugin on the PGM (Life Technologies) and with our MSKCC custom pipeline. For the MSK-IMPACT assay, the detailed procedure has been previously described.(19)

RESULTS

Sample characteristics

A total of 25 BAs from 21 patients were identified. The clinicopathologic findings are summarized in Table 1. Of 25 lesions, 11 were identified prospectively from routine clinical cases at MSKCC in 2016–2017 and 7 prospectively from the consultation practice of one of the authors (WDT) during the same period. One additional consult case and two archival cases were identified retrospectively at MSKCC, and another 4 were provided by contributors from other institutions. The original diagnoses included CMPT (n=15), peripheral glandular papilloma (n=3), adenocarcinoma in situ (AIS; n=3), nodular peribronchiolar metaplasia (PBM; n=2), atypical adenomatous hyperplasia (AAH; n=1), and basal cell hyperplasia (n=1).

The specimens harboring BAs included wedge resections (n=20) and lobectomies (n=5). For 10 patients, the surgical procedure was performed for BAs as the sole lesion (n=10), whereas 11 patients had other lung lesions resected in the same procedure in addition to BA, including primary lung adenocarcinoma (n=12), metastatic renal cell carcinoma (n=2), and necrotizing granuloma (n=1). Six BAs were not seen on imaging studies and represented incidental findings grossly (n=2) or microscopically (n= 4) in specimens resected for other lesions. Of patients with BAs and concurrent lung adenocarcinomas, 3 patients had

multifocal AAH and AIS. Three patients (14%) had more than 1 BA (2 in two patients; 3 in one patient).

Patient Characteristics and Radiologic Features

The patients were 11 men and 10 women with a median age of 72 (range: 55 to 83 years). The majority of patients (75%) had a history of smoking. Twelve patients (83%) were Caucasian, 2 (17%) were Asian, and no ethnicity information was available in 7 patients.

Computed tomography (CT) imaging studies were available for 14 lesions in 12 patients. Radiologically, BAs appeared as peripheral solid (n=8), ground-glass (n=4) or mixed solid/ground glass nodules (n=2). Radiologic tumor size was on average 0.6 cm (range: 0.2 to 1.1 cm). Positron emission tomography (PET) scan was available for two lesions; one showed a standardized uptake value (SUV) of 1.6 while another showed no FDG avidity. In patients who were followed with serial CTs prior to resection (n=6), four patients had tumors that remained stable in size during a period of 4–14 months, whereas two patients had lesions that showed 1 mm growth in 5 months and 3 mm in 2 years, respectively.

Clinical follow-up was available in 12 patients with a median follow-up interval of 11 months (range: 1 month to 9 years). None of the patients had local recurrences or distant metastases.

Gross findings

Grossly, most BAs appeared as well-circumscribed tan-white to grey firm nodules, some with a mucoid appearance. The median gross tumor size was 0.5 cm (range: 0.2 to 2.0 cm). In a minority of cases (n=4), small lesions were not identified on gross examination and were only noted microscopically (microscopic size 0.15 to 0.3 cm).

Histologic and Immunohistochemical Findings

All BAs were peripheral in location, distinctly nodular, and unassociated with bronchial lumens. The tumors were invariably adjacent to bronchioloarterial bundles or penetrated by unpaired medium-sized arteries, supporting their peribronchiolar location. In addition, all tumors were composed of bilayered cellular proliferation with a continuous basal cell layer, highlighted by basal cell markers p40 and/or CK5/6 (confirmed in all cases). The lesional cells showed no cytologic atypia or increased mitotic activity in any cases.

The tumors showed a spectrum of morphologic and immunohistochemical findings which we categorized into two main groups – proximal (n=8) and distal (n=17) based on the morphologic and immunohistochemical similarity with the proximal and distal portions of normal bronchiolar structures, as detailed below.

Eight proximal-type BAs (32%) recapitulated morphologic and immunohistochemical features of proximal bronchiolar epithelium and were composed of abundant mucinous and ciliated cells with subjacent basal cells. They showed a spectrum of architectural patterns that ranged from predominantly papillary in four cases to predominantly flat in the other four cases. The cases with predominant papillary architecture met all major diagnostic features of prototypical CMPTs (Figure 1). In such cases, the morphologic features were

virtually identical to those of glandular papillomas extending into alveolar lung tissue with the exception that these tumors were not endobronchial in location but rather situated on alveolar walls. By comparison, the other four cases shared only partial features with CMPTs in terms of cellular composition; architecturally, they were predominantly flat and proliferated along the scaffolding of native alveolar walls (Figure 2), although focal papillae could be found in 3 cases. TTF1 staining in luminal cells was completely negative in five cases (Figure 2) and weakly/focally positive in two other cases (Figure 1). TTF1 staining in basal cells showed weak/focal positivity in five cases (Figure 1 and 2) and negative immunoreactivity in two other cases.

Seventeen distal-type BAs (68%) resembled morphologic and immunohistochemical characteristics of distal respiratory bronchiolar epithelium. Of these, 13 cases contained only focal mucin and/or cilia, and the predominant cell type overlying the basal cell layer was a population of cuboidal cells that resembled type II pneumocytes (Figure 3). In addition, a minority of cells showed apical cytoplasmic snouts resembling club (Clara) cells. When present, focal mucinous cells resided in distinctive glandular crypts (Figure 3B), and focal ciliated cells were present as peculiar micropapillary tufts (Figure 3C and 3D). Four remaining distal-type cases completely lacked any ciliated or mucinous cells. They were characterized by bilayered epithelium comprising basal cells and luminal cuboidal and club cells (Figure 4). All 17 distal-type lesions were entirely or predominantly flat, and given the absence or paucity of mucinous cells, these tumors did not exhibit any significant extracellular mucin production. TTF1 was performed on 12 of 17 distal-type BAs, and showed diffuse positivity in both luminal and basal cells in all cases tested. A subset of these cases (n=4) was also stained for Napsin A, showing labeling in luminal cells in all cases (Figure 4). CC10, a marker of club cells, was performed in selected cases of distal-type BAs showing patchy positivity in a subset of luminal cells, confirming club cell differentiation (Figure 4 Inset).

Additional notable microscopic features in both subtypes of BAs included frequent admixture of stromal lymphoplasmacytic infiltrate (n=18). Seemingly discontinuous skip growths composed of sharply demarcated strips of tumor cells, analogous to skip lesions of invasive mucinous adenocarcinoma (IMA), were observed in nine cases (Figure 5A); these were seen in both proximal and distal-type lesions. Another notable feature in both types of lesions was apparent detachment of ciliated micropapillary tufts into alveolar spaces. This was seen at least focally in 7/8 proximal-type and 5/17 distal-type lesions; in two lesions, this feature was so extensive that it simulated the appearance of micropapillary adenocarcinoma (Figure 5B). Although no definite stromal invasion or desmoplasia was identified in any cases, 8 cases exhibited focal stromal expansion leading to acinar-like appearance of alveolar walls (Figure 5C). Squamous metaplasia of basal cells, reminiscent of mixed squamous and glandular papillomas, was seen in two cases (Figure 5D).

To compare the staining profiles of BAs to that of normal airways, staining of normal lung tissue was reviewed in histological sections from 15 patients. Similar to proximal-type BAs, luminal cells in proximal bronchioles were largely negative for TTF1, with only focal weak labeling in some areas (Figure 7). In contrast, similar to distal-type BAs, small respiratory bronchioles showed frequent TTF1 positivity in luminal cells (Figure 7). CC10 highlighted

occasional club cells within respiratory bronchioles (not shown). All airways showed a continuous basal cell layer, highlighted by p40 and CK5/6. TTF1 was occasionally co-expressed with p40 and CK5/6 in basal cells: labeling was weak in proximal bronchioles but stronger in distal bronchioles (Figure 7). Napsin A was largely negative in proximal and distal airways; however, rare distal bronchioles with patches of Napsin A-positive cells overlying basal cells were identified (Supplementary Figure 1), analogous to the staining profile of distal-type BAs. In addition, staining of lung tissue with interstitial lung disease and peribronchiolar metaplasia (PBM) was performed for comparison, revealing frequent positivity for TTF1 and patchy positivity for Napsin A in luminal cells. Patient characteristics and tumor size associated with proximal vs distal-type BAs is summarized in Table 3, and revealed no significant differences.

Frozen Section Interpretation

Intraoperative frozen sections were performed on nine cases, and the rendered diagnoses included adenocarcinoma (n=7) and mucous gland adenoma (n=1) [Table 1].

Molecular Findings

NGS was successfully performed in 19 BAs. In addition, BRAF V600E IHC was performed on 4 cases lacking sequencing data. Overall, combining sequencing and IHC data, driver mutations were identified in 18 of 21 BAs, including *BRAF* (n=8, 38%), *KRAS* (n=5, 24%), *EGFR* (n=4, 20%), and *HRAS* (n=1, 5%) (Table 2; Figure 8A).

Driver mutations identified by sequencing (n=16) included *BRAF* (n=6), *EGFR* (n=4), *KRAS* (n=5), and *HRAS* (n=1). All *BRAF* driver mutations were *BRAF* c.1799T>A (p.V600E). *EGFR* alterations included two cases with unusual exon 19 deletions (p.E746_S752>V and p.L747_S752del) and two cases with exon 20 insertions (p.D770_N771insNPH [alternative annotation: p.N771_H773dup]). In addition, the case with p.L747_S752del also harbored a concurrent p.D761Y mutation. All *KRAS* mutations were missense mutations involving codon 12 (two p.G12V, two p.G12D, and one p.G12C), while the single case with *HRAS* mutation was a p.G13R. All the driver mutations were mutually exclusive. The total number of mutations per case was low (range: 1 to 2). Eleven cases had the driver mutation as the sole genomic abnormality. Notably, none of the cases with *BRAF* or *EGFR* driver mutations (n=10) harbored any mutations outside the driver genes. By comparison, 4 of 6 cases with *KRAS* or *HRAS* driver mutations were found to have an additional mutation per case.

In addition, BRAF V600E IHC was performed concurrently with sequencing on 19 cases, and molecular results and IHC were concordant in all cases (6 positive, 13 negative). Importantly, BRAF V600E IHC labeled both basal cells and luminal cells in all positive cases (Figure 8C). ALK (D5F3) stain was performed on 3 cases lacking a detectable driver mutation, and all were negative.

For proximal versus distal-type BAs, the frequency and spectrum of mutations were comparable (Table 2). Driver mutations were present in 5/8 (62.5%) of proximal-type and 13/13 (100%) of distal-type BAs (Table 2). The lower rate of driver mutations in proximal-type BAs was not statistically significant (p=0.73). *BRAF* mutations were more common in

distal-type lesions compared to proximal (54% vs 13%, respectively), but this was not statistically significant (p=0.37). Furthermore, no apparent morphologic associations were seen with any of the above driver mutations.

Molecular Studies on Patients with Multiple BAs or BAs and Carcinomas in the Same Patient

In patients with more than one BA (n=3), molecular testing of all lesions was performed. The molecular profiles of BAs were different in two patients. The third patient had two morphologically distinct BAs, both of which harbored *BRAF* V600E mutations (Table 2).

Eight patients with BAs had concurrent lung adenocarcinomas. Five of these lung adenocarcinomas underwent NGS studies, and in all cases, the molecular profiles were entirely distinct from the BAs (Table 2).

DISCUSSION

This study describes a family of lesions that we have designated as bronchiolar adenomas, which are unified histologically by bilayered bronchiolar-type proliferation with a continuous layer of basal cells (p40 and CK5/6-positive), recapitulating various levels of the bronchiolar tree. On morphologic and immunohistochemical grounds, we divided BAs into proximal and distal types based on similarities to respective portions of bronchiolar tree. As such, luminal cells in proximal-type BAs contained abundant ciliated and mucinous cells, and were either negative or weakly/focally positive for TTF1, similar to proximal bronchiolar epithelium. In contrast, distal-type BAs were composed of predominantly non-ciliated cuboidal cells (TTF1+) and scattered club/Clara cells (CC10+) with scant to absent mucinous and ciliated cells, resembling the composition and immunoprofile of constituent cells in terminal bronchioles (see Figure 9).(20, 21) Even though Napsin A is not widely known to be expressed in distal airways, we found that focal labeling can occur in occasional luminal cells in terminal bronchioles. Thus, the peculiar phenotype of TTF1/Napsin A-positive luminal cells overlying basal cells in distal BAs may mirror differentiation in a subpopulation of cells in distal airways. We also note that the division of proximal vs distal BAs was not entirely dichotomous; for a subset of lesions, the designation reflected the predominant histology, as lesional cells showed focal differentiation toward the other portions of the bronchiolar tree. Thus, based on morphologic grounds, our findings suggest that BAs exhibit a morphologic spectrum reflecting differentiation toward either the proximal or distal bronchiole, and some cases show minor overlap. Our histopathologic conclusion regarding the nosologic relationship of these lesions is supported by their shared genomic profiles, as discussed further below.

An important consideration for the concept of bronchiolar adenomas is their relationship with CMPTs. In our series, only a subset of proximal-type BAs had prominent papillary architecture and would fit the classic description of CMPT; other proximal-type cases were entirely or predominantly flat, thus sharing only partial features with CMPTs. Conversely, the morphologic features of distal-type lesions were incompatible with the description of CMPT, in that they had minimal or complete absence of ciliated and mucinous cells, as well as absence of papillae. Given the partially overlapping morphology and similar genomic

profiles, we propose that lesions currently designated as CMPT represent a subset of proximal-type BAs. We believe that the term of CMPT is too restrictive to reflect the full morphologic spectrum of the family of lesions described here, and introduction of the term of bronchiolar adenoma may facilitate their wider recognition.

While the majority of CMPTs have been described in patients from East Asian countries,(4–18) only a handful of cases in non-Asian patients have been previously documented.(14) Our study, on the other hand, consists of predominantly Caucasian patients. It remains unknown whether ethnic predisposition truly exists for this family of lesions, or if the lower incidence in Western countries is due to under-recognition and underdiagnosis. Our data suggest that this family of lesions may not be as rare as they are currently believed, as over two-thirds of the cases in this study were prospectively identified over the span of one year after we recognized the morphologic spectrum of these lesions.

The central arguments for the recognition of BAs as a distinct entity is to promote their distinction from conventional adenocarcinomas, which they may morphologically mimic. The distinction from adenocarcinoma is crucial as BAs behave in an indolent fashion with no recurrences and metastases reported to date (4–18) and none observed in our study. The differential diagnosis varies with the subtype of BAs. For proximal-type BAs with prominent mucinous features, the main differential diagnosis is with invasive mucinous adenocarcinomas (IMA). The growth pattern over alveolar walls, presence of skip lesions, and abundance of secreted mucin and mucinous cells in these lesions underline the striking morphologic similarities with IMAs, which are typically also morphologically bland. The key to distinguishing these lesions is the recognition of a continuous basal cell layer, which in well-processed sections can be at least suspected morphologically, followed by confirmation by IHC for basal cell markers (p40/p63, CK5/6), if necessary. In addition, the presence of ciliated cells would also support the diagnosis of BA over IMA. Another helpful distinguishing feature is size: virtually all BAs are small lesions (≤2 cm), whereas IMAs vary in size but can form large consolidative masses. The fact that BAs can form apparently discontinuous skip lesions analogous to IMAs is peculiar for putatively benign lesions. Unlike IMAs, these skip lesions do not extend away from the main tumor for more than a few alveoli. We hypothesize that the seemingly discontinuous spread may represent lesional cells being interconnected with each other in three-dimensional spaces and not well visualized in two-dimensional histologic preparations.

The second major differential diagnosis is with adenocarcinoma with micropapillary pattern, since a subset of BAs exhibit prominent intraluminal micropapillary tufts (see Figure 5B). In fact, 2 lesions in this study were submitted for consultation with the diagnostic consideration of a peculiar micropapillary adenocarcinoma. However, the presence of apical cilia can be readily appreciated on high-power examination of the micropapillary tufts in BAs, along with the presence of a basal cell layer, facilitating this distinction.

While distinguishing BA from adenocarcinoma is relatively straightforward in permanent sections once this diagnosis is considered, BAs submitted for frozen sections can represent an extremely difficult diagnostic pitfall even for experienced thoracic pathologists (see Figure 6A). The high rate of misinterpreting BAs as adenocarcinomas on frozen sections

(7/9 in this series), also noted previously for CMPTs,(15) can be partially attributed to the relatively uncommon nature of this entity and lack of familiarity with this family of tumors. More importantly, many morphologic features of BAs are difficult to recognize on frozen sections due to poor tissue fixation. Most notably, apical cilia often appear as indistinct, ruffled borders and can be nearly impossible to visualize on frozen section slides, even when the slides are retrospectively reviewed at high magnification (see Figure 6B). In addition, it is not possible to rely exclusively on the presence of cilia to arrive at this diagnosis, as a significant proportion of distal BAs do not contain cilia. The most reliable diagnostic clue in the frozen section setting is thus the recognition of a continuous basal cell layer, which is universally present in all BAs and consistently absent in lung adenocarcinomas (NR, JC – personal observations). Awareness of this diagnostic possibility and careful search for basal cells can lead to the correct diagnosis and avoid overtreatment.

While there are reports of “ciliated adenocarcinoma” in the literature,(22) to our knowledge, basal cell markers were not tested in those cases. It is possible that those entities represented proximal-type BAs. In fact, one case in our series was identified by retrospective re-review of a case initially classified as ciliated adenocarcinoma.

On the other end of the spectrum, the differential diagnostic considerations for distal-type BAs with predominantly flat architecture and sparse mucin can include reactive proliferations known as peribronchiolar metaplasia (PBM) or Lambertosis. Peribronchiolar metaplasia is a relatively common histologic finding often occurring in the setting of interstitial lung disease, comprising a proliferation of distal bronchiolar-type epithelium without cytologic atypia over alveolar parenchyma.(23) Distal-type BA and PBM share many histologic features, including peribronchiolar localization, bilayered nature with underlying basal cells and luminal ciliated cells, and occasional foci of mucinous cells.(24, 25) In line with this morphologic similarity, several distal-type BAs were previously diagnosed as “nodular PBMs” in our practice. Histologic features that support the diagnosis of BA include a solitary, well-circumscribed lesion with a distinctly nodular contour, relatively unremarkable background lung, and presence of ciliated cells on micropapillary tufts or in peculiar outpouchings (see Figure 5B). By contrast, PBMs tend to show ill-defined borders and are often accompanied by interstitial fibrosis and organizing pneumonia.(25) In addition, PBM is usually a multifocal process with many airways involved, often to a similar degree, especially in the setting of small airways disease or interstitial lung disease. Nevertheless, in a small wedge resection, this distinction can be difficult or impossible. The demonstration of driver mutations, such as *BRAF* or *EGFR*, supports that BAs are distinct entities from PBMs. We performed BRAF IHC on 9 PBMs, and none showed positive labeling (data not shown). However, unlike the clear importance of distinguishing BAs from adenocarcinomas, the distinction of distal-type BA and PBM does not appear to be critical from an oncologic perspective since both are putatively benign lesions. Thus, we do not advocate routine use of BRAF IHC or molecular testing to make this distinction. In equivocal cases, the diagnosis of “nodular bronchiolar-type proliferation” may be sufficient for practical purposes.

While this study solely consisted of BAs from resection specimens, given the peripheral location of these lesions, they may be amenable to percutaneous CT-guided core biopsy or

fine needle aspiration. As in resections, the differential diagnosis on small specimens would depend on the specific subtype of BA and the type of sampling involved. For cytology specimens, recognition of ciliated cells in proximal-type cases would likely lead to a benign diagnosis. However, distal-type cases entirely devoid of ciliated cells could represent potential diagnostic pitfall raising consideration for a well-differentiated adenocarcinoma. For core biopsy specimens, distinction from adenocarcinoma can be accomplished by recognizing the ciliated cells and/or bilayered nature of the lesion and performing basal cell markers for confirmation. Distinguishing distal-type BAs from PBM on a limited sample may not be possible, but clinicoradiologic correlation may be helpful to confirm the discrete nature of the sampled lesion.

Proximal-type BAs with papillary architecture (encompassing prototypical CMPTs) and endobronchial glandular papillomas share many morphologic similarities, and the relationship between the two entities has been subject to ongoing debate. Glandular (or mixed squamous cell and glandular) papillomas are by definition endobronchial in nature according to the current World Health Organization (1) classification. While papillomas are by definition endobronchial in location, extension of papillomas into peripheral lung is a well-known phenomenon.(26) Thus, the diagnosis of proximal-type BAs requires the exclusion of an adjacent endobronchial component. Prior to the recognition of CMPT as a discrete diagnostic entity, peripheral glandular papilloma-like lesions without an endobronchial component have been reported over the years under the terms of “peripheral papilloma,” “solitary peripheral ciliated glandular papilloma,” and “peripheral pulmonary papillary/glandular neoplasm with ciliated cells.”(27–31) We believe that except for the location, glandular papillomas and proximal-type BAs are virtually identical histologically, with one growing as an endobronchial lesion and the other growing peripherally on alveolar walls. Because of the rarity of papillomas, their molecular landscape has not been extensively characterized. Future studies investigating the presence of driver mutations in papillomas may further help elucidate the nosologic relationship between papillomas and BAs.

Genomic analyses from current and prior studies highlight the unique molecular profile of BAs, which are entirely distinct from lung adenocarcinomas; in addition, they underscore the similar molecular profiles of distal- and proximal-type BAs, including those with classic features of CMPT. The most prevalent genetic alterations in BAs involved *BRAF* (38%), *KRAS* (24%), *EGFR* (19%), and *HRAS* (5%), and the distribution of these mutations was similar in distal- and proximal-type BAs (Table 2). Furthermore, the frequency of driver mutations of BAs in our cohort (86%) is similar to that of CMPTs previously reported by Kamata et al,(10) who described *BRAF* V600E or *EGFR* deletions in 4 and 3 of 10 CMPTs, respectively. Overall, the presence of driver mutations supports the neoplastic, clonal nature of BAs, and the similarity of mutations across the morphologic spectrum of the described lesions supports their nosologic relationship. The apparent enrichment of *BRAF* V600E mutations in distal-type lesions in our series was not statistically significant, and it was similar to the prevalence of *BRAF* mutations in CMPTs in prior studies. It is nevertheless possible that some genomic differences could exist along the spectrum of BAs, and this will require further studies.

Similar to prior studies in CMPTs, we found *BRAF* V600E to be the single most common driver mutation in BAs. *BRAF* V600E driver mutations have been described in a variety of benign and malignant tumors, including Langerhans cell histiocytosis,(32) Erdheim-Chester disease,(33) metanephric adenomas of the kidney,(34) central nervous system gliomas,(35) hairy cell leukemia,(36) malignant melanoma,(37) colorectal carcinoma,(38, 39) and papillary thyroid carcinoma,(40) amongst others. Although *BRAF* mutations are present in 2.2% of lung adenocarcinomas,(41, 42) these adenocarcinomas often show micropapillary (43) and solid (44) predominant patterns and lack the bilayered growth pattern seen in BAs. As *BRAF* mutations can be seen in both benign and malignant lung tumors, the presence of *BRAF* mutations in BAs merely represents evidence for a neoplastic process and is not synonymous with malignancy.

We found the BRAF V600E immunohistochemical stain to show excellent concordance with NGS results. We also confirmed previous findings that the immunoreactivity was observed in both apical and basal cells,(10) supporting that the driver mutation was present in all cellular constituents within the lesion. One notable caveat is that staining for this marker is consistently seen in surface cilia;(10) therefore, clear cytoplasmic immunoreactivity away from the cilia is required for interpreting a true positive result.

KRAS mutations were the second most common driver mutations in BAs. A single case of *KRAS*-mutant CMPT was recently reported in the literature.(18) The current study shows that *KRAS* mutations are relatively common in BAs (24%). In addition, a single BA was found to have an *HRAS* G13R hotspot mutation co-occurring with a *BRAF* G464V mutation. Since non-V600E *BRAF* mutations have been described as concurrent mutations in the setting of other stronger driver mutations in the MAPK pathway,(44) the *HRAS* mutation was regarded as the primary mitogenic driver event in that case. Interestingly, the missense mutations in *KRAS*- or *HRAS*-mutant cases were predominated by transversion mutations, which are characteristic of tobacco-related carcinogenic signature.(45) Perhaps not surprisingly, five of six patients with *KRAS*- or *HRAS*-mutant tumors had a history of cigarette smoking.

EGFR deletions/insertions represented the third most prevalent driver alteration, seen in 19% of BAs in our cohort. Given that the *EGFR* exon 19 deletions identified in BAs, p.E746_S752>V and p.L747_S752del, are rare variants distinct from common sensitizing exon 19 deletions, we wanted to determine the prevalence of such alterations in lung adenocarcinoma. We therefore queried the data on 2809 lung adenocarcinomas from the MSK-IMPACT Clinical Sequencing Cohort in the cBioPortal database.(19, 46–48) Of those cases, 841 (29.9%) tumors harbored *EGFR* mutations, and exon 19 deletions matching those seen in BAs occurred in only 19 (2.2%) and 4 (0.5%) of *EGFR*-mutant lung adenocarcinomas, respectively. Importantly, one of *EGFR* deletions - p.E746_S752delinsV - is identical to the variant reported in a prior CMPT study,(10) further underscoring the similarities in the molecular landscape of BAs and tumors designated as CMPTs. Similarly, we found that the *EGFR* exon 20 insertions involving p.D773_N774insNPH (p.N771_H773dup) identified in two BAs in our series, represented rare variants reported in the literature and occurred in only 4 (0.5%) of *EGFR*-mutant lung adenocarcinoma in the cBioPortal database.(19, 46, 47, 49, 50) Overall, the predilection for uncommon *EGFR*

deletions/insertions in the absence of common variants in BAs reinforces their highly distinctive biology from adenocarcinomas. This is further supported by the finding that most putative drivers in BAs were present as a solo alteration, which is distinctly uncommon for adenocarcinomas.(46–48) Interestingly, the exact *EGFR* exon 20 insertion has been recently described in a high proportion of inverted sinonasal papillomas,(51) further raising the nosologic relationship between BAs and papillomas.

Molecular studies on patients with multiple BAs or BAs with concurrent lung adenocarcinomas were helpful in establishing clonal relationships among multiple tumors. In patients with BAs and concurrent adenocarcinomas, the mutational profiles of the BAs were entirely distinct from the adenocarcinomas, supporting that the foci of BAs did not represent peculiar intrapulmonary spread from the adenocarcinoma. By contrast, three patients had multiple BAs, a phenomenon that has not been described previously in CMPTs. The presence of distinct driver mutations in individual lesions in the first two patients confirms that the lesions were not clonally related, whereas the presence of identical *BRAF* V600E mutations in the last patient could be coincidental given that *BRAF* is the most common genetic alteration in these lesions. We also identified three patients in whom BAs were present in the background of adenocarcinomas with multifocal AAH and AIS; these patients were smokers, further raising the possibility that smoking may predispose to the formation of BAs.

Given the bland cytology and absence of disease recurrences in the prior (4–18) and current studies, BAs appear to be benign adenomatous growths. Rare reports of adenocarcinoma occurring in association with CMPTs have been described in two studies.(11, 29) One study described a CMPT with concomitant colloid adenocarcinoma;(11) however, basal cell markers were not performed in the study to confirm the presence of basal cells in the CMPT component. The other study demonstrated attentuated p63 immunoreactivity suggestive of invasive foci in two cases.(29) However, typical histologic features associated with malignancy, such as cytologic atypia, necrosis, or increased mitotic activity, were not seen in any of the cases described in the aforementioned study. Nonetheless, we cannot exclude the possibility that progression/malignant transformation may occur in rare cases of BA/CMPTs; further study of these lesions and continued follow-up are required to address the full biologic potential of BAs.

In conclusion, our clinical, morphologic, and molecular data suggest that adenomas derived from bronchiolar epithelium encompass a spectrum of lesions beyond the current concept of CMPTs, warranting a change in terminology. We believe that lesions currently designated CMPTs represent a subgroup of these lesions, and we propose the term bronchiolar adenoma to encompass the broad morphologic spectrum of this family of neoplasms.

Supplementary Material

Refer to Web version on PubMed Central for supplementary material.

ACKNOWLEDGMENTS

The authors thank Dr. Akihiko Yoshida at National Cancer Center Hospital, Tokyo, Japan, for reviewing the manuscript pre-submission and providing helpful comments and feedback. We also thank Julie Intrieri at MSKCC for her assistance with the Ampliseq assay.

Source of Funding: Supported in part by a Memorial Sloan Kettering Cancer Center Department of Pathology Research and Development grant (to NR). The MSK-IMPACT program is supported in part by NIH P01 CA129243 (ML, LB, NR), NIH P30 CA008748 (MSKCC), the Marie-Josée and Henry R. Kravis Center for Molecular Oncology at MSKCC, and Cycle for Survival.

REFERENCES

1. Travis WD, Brambilla E, Burke A, et al. WHO classification of tumours of the lung, pleura, thymus and heart. International Agency for Research on Cancer; 2015.
2. Miller RR. Bronchioloalveolar cell adenomas. Am J Surg Pathol. 1990;14:904–912. [PubMed: 2403196]
3. Toker C. Observations on the ultrastructure of a bronchial adenoma (carcinoid-type). Cancer. 1966;19:1943–1948. [PubMed: 5927947]
4. Ishikawa Y. Ciliated muconodular papillary tumor of the peripheral lung: benign or malignant? Pathol Clin Med (Byouri-to-Rinsho). 2002;20:964–965.
5. Harada T, Akiyama Y, Ogasawara H, et al. Ciliated muconodular papillary tumor of the peripheral lung: A newly defined rare tumor. Respiratory Medicine CME. 2008;1:176–178.
6. Sato S, Koike T, Homma K, et al. Ciliated muconodular papillary tumour of the lung: a newly defined low-grade malignant tumour. Interact Cardiovasc Thorac Surg. 2010;11:685–687. [PubMed: 20724424]
7. Hata Y, Yuasa R, Sato F, et al. Ciliated muconodular papillary tumor of the lung: a newly defined low-grade malignant tumor with CT findings reminiscent of adenocarcinoma. Jpn J Clin Oncol. 2013;43:205–207. [PubMed: 23275641]
8. Chuang HW, Liao JB, Chang HC, et al. Ciliated muconodular papillary tumor of the lung: a newly defined peripheral pulmonary tumor with conspicuous mucin pool mimicking colloid adenocarcinoma: a case report and review of literature. Pathol Int. 2014;64:352–357. [PubMed: 25047506]
9. Kamata T, Yoshida A, Kosuge T, et al. Ciliated muconodular papillary tumors of the lung: a clinicopathologic analysis of 10 cases. Am J Surg Pathol. 2015;39:753–760. [PubMed: 25803171]
10. Kamata T, Sunami K, Yoshida A, et al. Frequent BRAF or EGFR Mutations in Ciliated Muconodular Papillary Tumors of the Lung. J Thorac Oncol. 2016;11:261–265. [PubMed: 26718882]
11. Ishikawa M, Sumitomo S, Imamura N, et al. Ciliated muconodular papillary tumor of the lung: report of five cases. J Surg Case Rep. 2016;2016.
12. Kon T, Baba Y, Fukai I, et al. Ciliated muconodular papillary tumor of the lung: A report of five cases. Pathol Int. 2016;66:633–639. [PubMed: 27671838]
13. Lau KW, Aubry MC, Tan GS, et al. Ciliated muconodular papillary tumor: a solitary peripheral lung nodule in a teenage girl. Hum Pathol. 2016;49:22–26. [PubMed: 26826405]
14. Liu L, Aesif SW, Kipp BR, et al. Ciliated Muconodular Papillary Tumors of the Lung Can Occur in Western Patients and Show Mutations in BRAF and AKT1. Am J Surg Pathol. 2016;40:1631–1636. [PubMed: 27454941]
15. Chu HH, Park SY, Cha EJ. Ciliated muconodular papillary tumor of the lung: The risk of false-positive diagnosis in frozen section. Human Pathology: Case Reports. 2017;7:8–10.
16. Jin Y, Shen X, Shen L, et al. Ciliated muconodular papillary tumor of the lung harboring ALK gene rearrangement: Case report and review of the literature. Pathol Int. 2017;67:171–175. [PubMed: 28150468]
17. Taguchi R, Higuchi K, Sudo M, et al. A case of anaplastic lymphoma kinase (ALK)-positive ciliated muconodular papillary tumor (CMPT) of the lung. Pathol Int. 2017;67:99–104. [PubMed: 28093881]

18. Udo E, Furusato B, Sakai K, et al. Ciliated muconodular papillary tumors of the lung with KRAS/BRAF/AKT1 mutation. Diagn Pathol. 2017;12:62. [PubMed: 28830562]
19. Zehir A, Benayed R, Shah RH, et al. Mutational landscape of metastatic cancer revealed from prospective clinical sequencing of 10,000 patients. Nat Med. 2017;advance online publication.
20. Nakajima M, Kawanami O, Jin E, et al. Immunohistochemical and ultrastructural studies of basal cells, Clara cells and bronchiolar cuboidal cells in normal human airways. Pathol Int. 1998;48:944–953. [PubMed: 9952338]
21. Yatabe Y, Mitsudomi T, Takahashi T. TTF-1 expression in pulmonary adenocarcinomas. Am J Surg Pathol. 2002;26:767–773. [PubMed: 12023581]
22. Nakamura S, Koshikawa T, Sato T, et al. Extremely well differentiated papillary adenocarcinoma of the lung with prominent cilia formation. Acta pathologica japonica. 1992;42:745–750. [PubMed: 1466246]
23. Fukuoka J, Franks TJ, Colby TV, et al. Peribronchiolar metaplasia: a common histologic lesion in diffuse lung disease and a rare cause of interstitial lung disease: clinicopathologic features of 15 cases. Am J Surg Pathol. 2005;29:948–954. [PubMed: 15958861]
24. Tomashefski JF, Dail DH, Hammar SP. Dail and Hammar's pulmonary pathology. Nonneoplastic lung disease Vol. 1 Vol. 1. New York: Springer; 2008.
25. Leslie KO, Wick MR, Leslie KO. Practical pulmonary pathology : a diagnostic approach. 2018.
26. Wiatrak BJ, Wiatrak DW, Broker TR, et al. Recurrent Respiratory Papillomatosis: A Longitudinal Study Comparing Severity Associated With Human Papilloma Viral Types 6 and 11 and Other Risk Factors in a Large Pediatric Population. The Laryngoscope. 2004;114:1–23.
27. Flieder DB, Koss MN, Nicholson A, et al. Solitary pulmonary papillomas in adults: a clinicopathologic and in situ hybridization study of 14 cases combined with 27 cases in the literature. Am J Surg Pathol. 1998;22:1328–1342. [PubMed: 9808125]
28. Aida S, Ohara I, Shimazaki H, et al. Solitary peripheral ciliated glandular papillomas of the lung: a report of 3 cases. Am J Surg Pathol. 2008;32:1489–1494. [PubMed: 18708941]
29. Arai Y, Shimizu S, Eimoto T, et al. Peripheral pulmonary papillary/glandular neoplasms with ciliated cells and a component of well-differentiated adenocarcinoma: report of three tumours. Histopathology. 2010;56:265–269. [PubMed: 20102406]
30. Inamura K, Kumasaka T, Furuta R, et al. Mixed squamous cell and glandular papilloma of the lung: a case study and literature review. Pathol Int. 2011;61:252–258. [PubMed: 21418399]
31. Emerson LL, Layfield LJ. Solitary peripheral pulmonary papilloma evaluation on frozen section: a potential pitfall for the pathologist. Pathol Res Pract. 2012;208:726–729. [PubMed: 23131661]
32. Badalian-Very G, Vergilio J-A, Degar BA, et al. Recurrent BRAF mutations in Langerhans cell histiocytosis. Blood. 2010;116:1919–1923. [PubMed: 20519626]
33. Haroche J, Charlotte F, Arnaud L, et al. High prevalence of BRAF V600E mutations in Erdheim-Chester disease but not in other non-Langerhans cell histiocytoses. Blood. 2012;120:2700–2703. [PubMed: 22879539]
34. Choueiri TK, Cheville J, Palescandolo E, et al. BRAF mutations in metanephric adenoma of the kidney. European urology. 2012;62:917–922. [PubMed: 22727996]
35. Schindler G, Capper D, Meyer J, et al. Analysis of BRAF V600E mutation in 1,320 nervous system tumors reveals high mutation frequencies in pleomorphic xanthoastrocytoma, ganglioglioma and extra-cerebellar pilocytic astrocytoma. Acta Neuropathologica. 2011;121:397–405. [PubMed: 21274720]
36. Tiacci E, Trifonov V, Schiavoni G, et al. BRAF mutations in hairy-cell leukemia. N Engl J Med. 2011;364:2305–2315. [PubMed: 21663470]
37. Maldonado JL, Fridlyand J, Patel H, et al. Determinants of BRAF mutations in primary melanomas. Journal of the National Cancer Institute. 2003;95:1878–1890. [PubMed: 14679157]
38. Davies H, Bignell GR, Cox C, et al. Mutations of the BRAF gene in human cancer. Nature. 2002;417:949–954. [PubMed: 12068308]
39. Tol J, Dijkstra JR, Klomp M, et al. Markers for EGFR pathway activation as predictor of outcome in metastatic colorectal cancer patients treated with or without cetuximab. European Journal of Cancer. 2010;46:1997–2009. [PubMed: 20413299]

40. Kimura ET, Nikiforova MN, Zhu Z, et al. High prevalence of BRAF mutations in thyroid cancer: genetic evidence for constitutive activation of the RET/PTC-RAS-BRAF signaling pathway in papillary thyroid carcinoma. Cancer research. 2003;63:1454–1457. [PubMed: 12670889]
41. Paik PK, Arcila ME, Fara M, et al. Clinical Characteristics of Patients With Lung Adenocarcinomas Harboring BRAF Mutations. Journal of Clinical Oncology. 2011;29:2046–2051. [PubMed: 21483012]
42. Villaruz LC, Socinski MA, Abberbock S, et al. Clinicopathologic features and outcomes of patients with lung adenocarcinomas harboring BRAF mutations in the Lung Cancer Mutation Consortium. Cancer. 2015;121:448–456. [PubMed: 25273224]
43. Marchetti A, Felicioni L, Malatesta S, et al. Clinical features and outcome of patients with non-small-cell lung cancer harboring BRAF mutations. J Clin Oncol. 2011;29:3574–3579. [PubMed: 21825258]
44. Kinno T, Tsuta K, Shiraishi K, et al. Clinicopathological features of nonsmall cell lung carcinomas with BRAF mutations. Annals of oncology : official journal of the European Society for Medical Oncology. 2014;25:138–142. [PubMed: 24297085]
45. Sun S, Schiller JH, Gazdar AF. Lung cancer in never smokers - a different disease. Nat Rev Cancer. 2007;7:778–790. [PubMed: 17882278]
46. Cerami E, Gao J, Dogrusoz U, et al. The cBio Cancer Genomics Portal: An Open Platform for Exploring Multidimensional Cancer Genomics Data. Cancer Discovery. 2012;2:401. [PubMed: 22588877]
47. Gao J, Aksoy BA, Dogrusoz U, et al. Integrative analysis of complex cancer genomics and clinical profiles using the cBioPortal. Science signaling. 2013;6:pl1.
48. Jordan EJ, Kim HR, Arcila ME, et al. Prospective Comprehensive Molecular Characterization of Lung Adenocarcinomas for Efficient Patient Matching to Approved and Emerging Therapies. Cancer Discovery. 2017.
49. Yamamoto H, Toyooka S, Mitsudomi T. Impact of EGFR mutation analysis in non-small cell lung cancer. Lung Cancer. 2009;63:315–321. [PubMed: 18760859]
50. Arcila ME, Nafa K, Chaft JE, et al. EGFR Exon 20 Insertion Mutations in Lung Adenocarcinomas: Prevalence, Molecular Heterogeneity, and Clinicopathologic Characteristics. Molecular cancer therapeutics. 2013;12:220–229. [PubMed: 23371856]
51. Udager AM, Rolland DCM, McHugh JB, et al. High frequency targetable EGFR mutations in sinonasal squamous cell carcinomas arising from inverted sinonasal papilloma. Cancer research. 2015;75:2600–2606. [PubMed: 25931286]

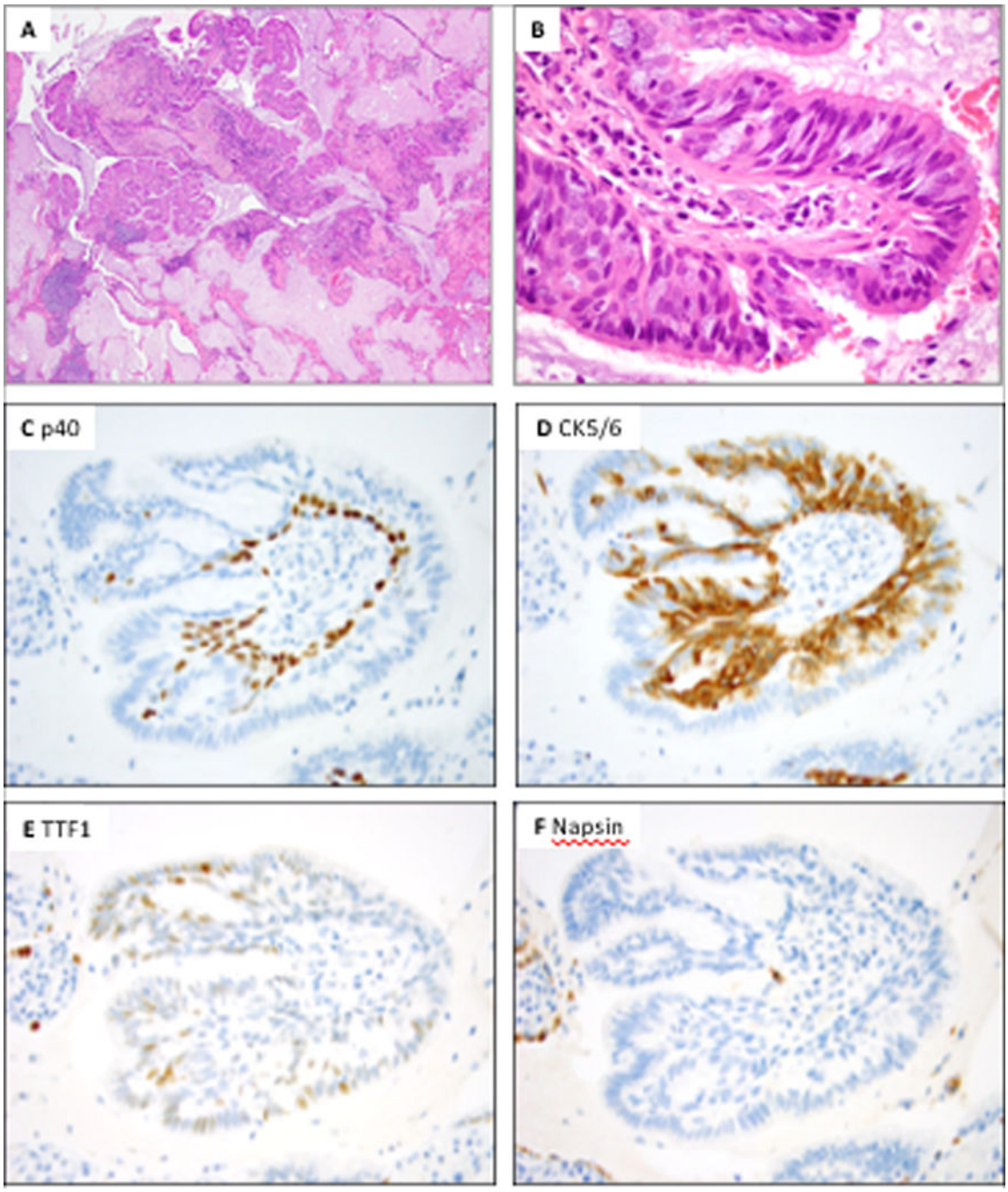

Figure 1.

Proximal-type bronchiolar adenoma with papillary architecture (Patient 4). A, At low power, the tumor shows prominent papillary architecture with abundant intra-alveolar mucin. B, At high power, the tumor shows predominance of ciliated and mucinous cells entirely surrounded by basal cells. C and D, P40 and CK5/6 highlight a continuous basal cell layer. E, TTF1 shows focal weak positivity in the basal cells and patchy variable positivity in the luminal cells. F, Napsin A is completely negative.

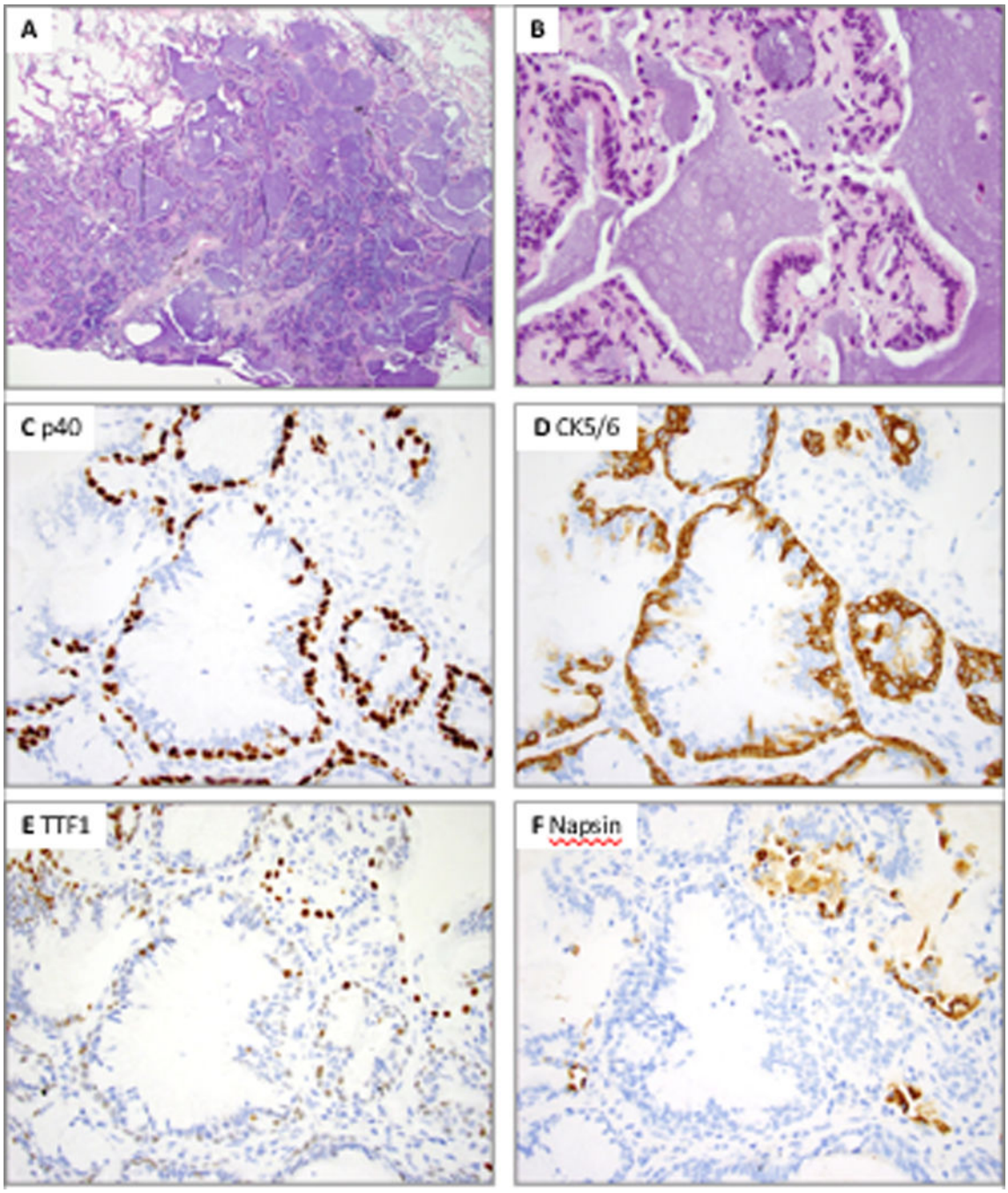

Figure 2.

Proximal-type bronchiolar adenoma with predominantly flat architecture (Patient 8, case 1). A, At low power, the tumor shows predominantly flat architecture with abundant intra-alveolar mucin. B, At high power, this tumor shows abundant ciliated and mucinous cells. C and D, P40 and CK5/6 highlight a continuous basal cell layer. E, TTF1 shows weak to moderate positivity in the basal cells, while it is negative in the luminal cells. F, Napsin A is completely negative; positive staining is seen in entrapped pneumocytes.

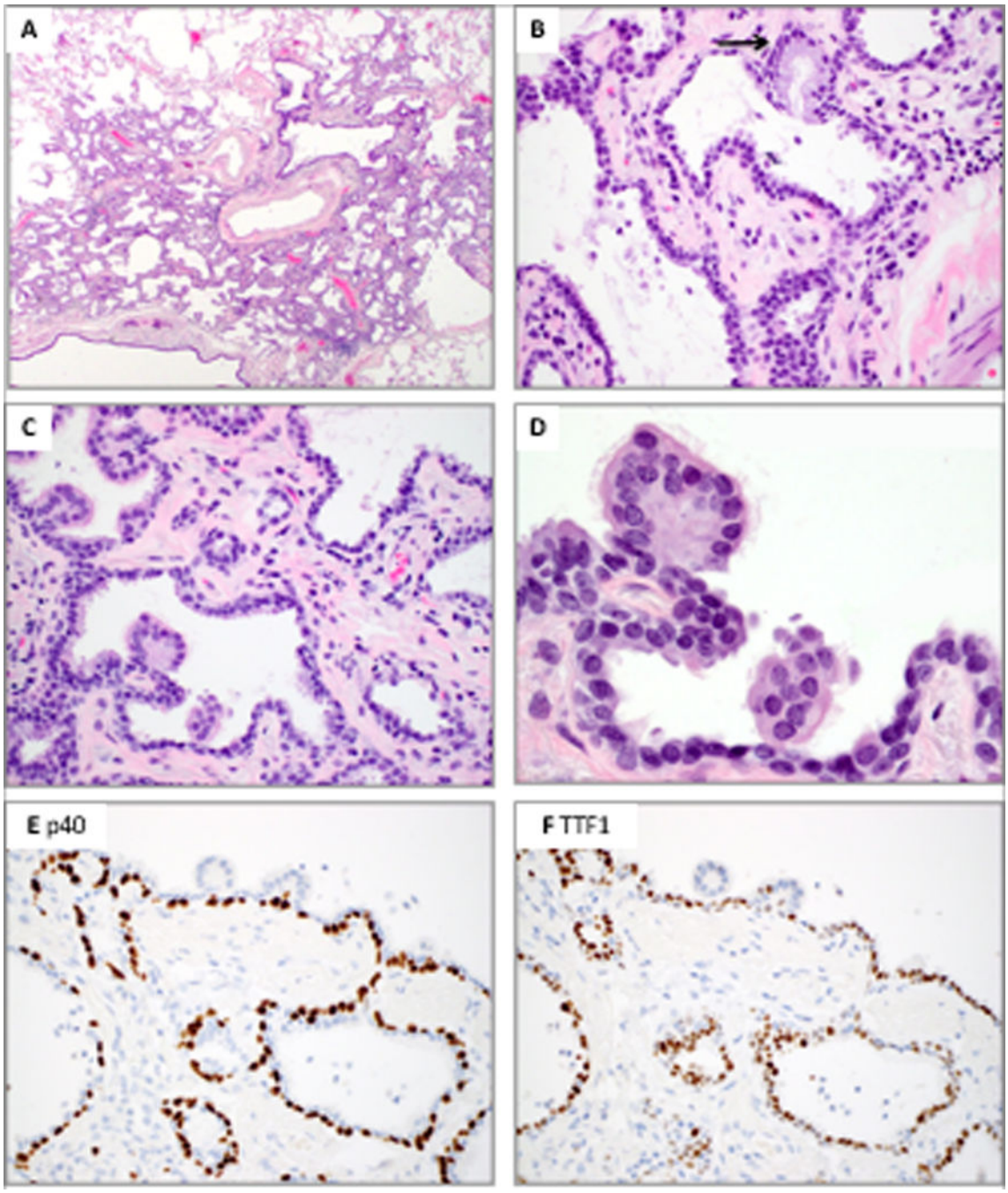

Figure 3.

Distal-type bronchiolar adenoma with entirely flat architecture and focal mucin and cilia (Patient 9, case 2). A, Low power shows peribronchiolar location penetrated by medium-sized muscular arteries. B, Mucinous cells are only present in rare glandular crypts (arrow). C and D, Ciliated cells are inconspicuous and only observed on top of micropapillary-like tufts. The luminal cells show predominance of cuboidal cells that resemble type II pneumocytes. E, P40 highlights a continuous basal cell layer. F, TTF1 is weakly positive in

the basal cells and moderately to strongly positive in non-ciliated luminal cuboidal cells; ciliated micropapillary tufts are negative.

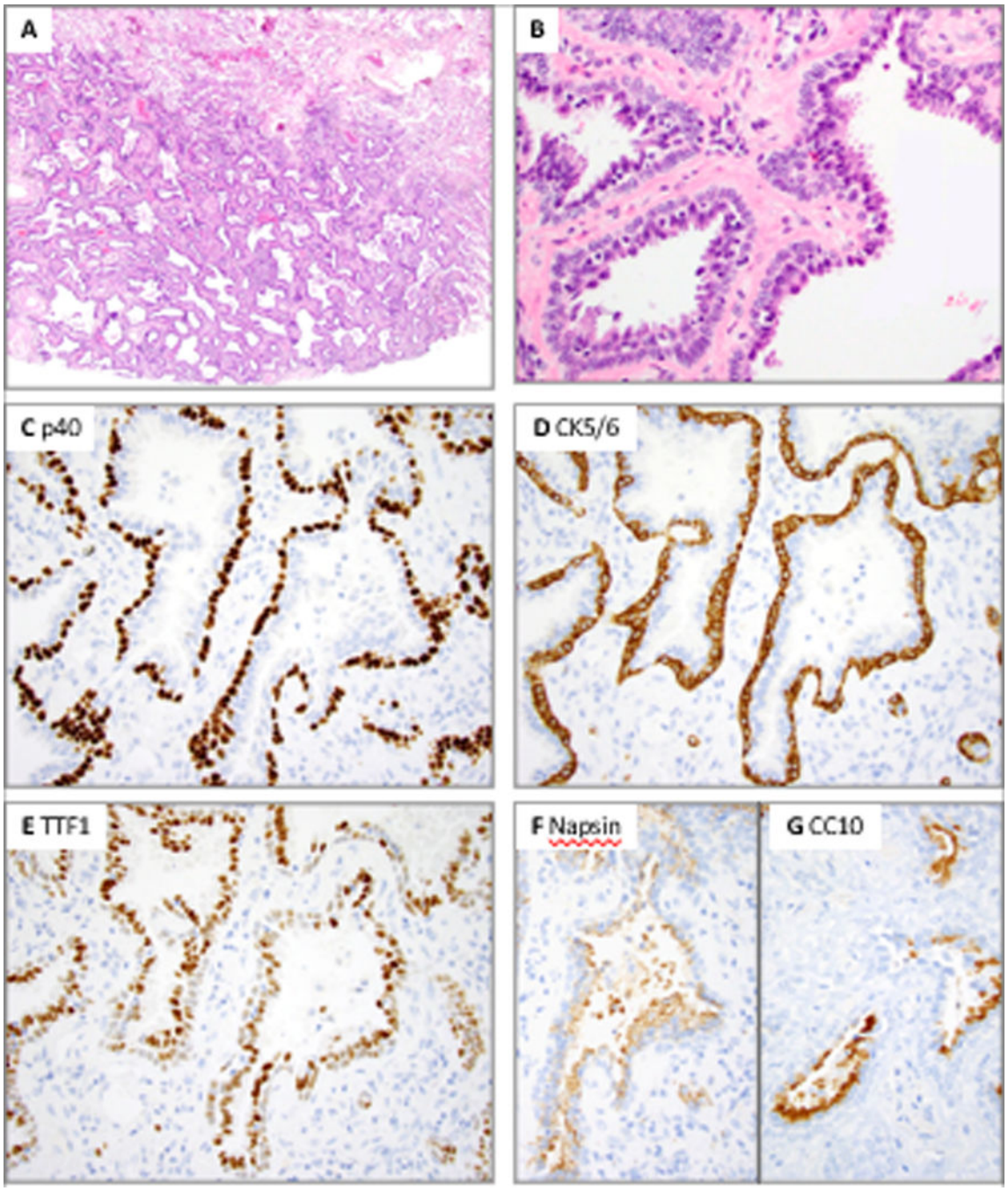

Figure 4.

Distal-type bronchiolar adenoma with entirely flat architecture and complete absence of mucinous and ciliated cells (Patient 8, case 2). A, Low power shows entirely flat architecture and sharply circumscribed contour from adjacent lung parenchyma. B, High power shows complete absence of mucinous and ciliated cells; some cells show apical cytoplasmic snouts resembling club cells. A dual layer with luminal and basal cells is apparent. C and D, P40 and CK5/6 highlight a continuous basal cell layer. E, F, G, TTF1 shows moderate to strong

positivity in luminal and weak positivity in basal cells, while Napsin A is positive in luminal cells only. Patchy CC10 positivity is seen in a subset of luminal cells.

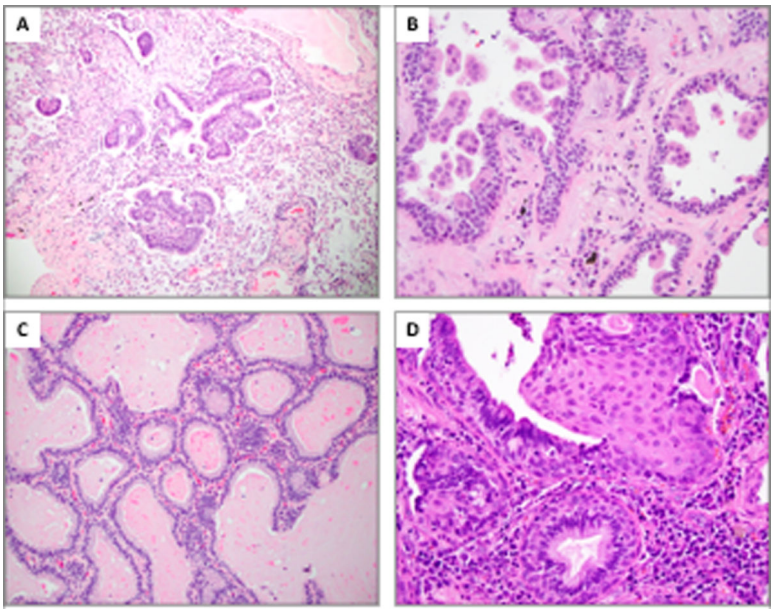

Figure 5.

Miscellaneous morphologic features in bronchiolar adenomas (BAs). A, A proximal-type BA shows seemingly discontinuous skip growths reminiscent of IMAs (Patient 3). B, A distal-type BA shows exuberant micropapillary-like tufts budding into alveolar spaces mimicking a micropapillary adenocarcinoma (Patient 10, case 1). C, A proximal-type BA shows flat architecture and focal stromal expansion that create an acinar-like appearance simulating an adenocarcinoma (Patient 5). D, A distal-type BA shows basal cell hyperplasia and overt squamous metaplasia (Patient 21).

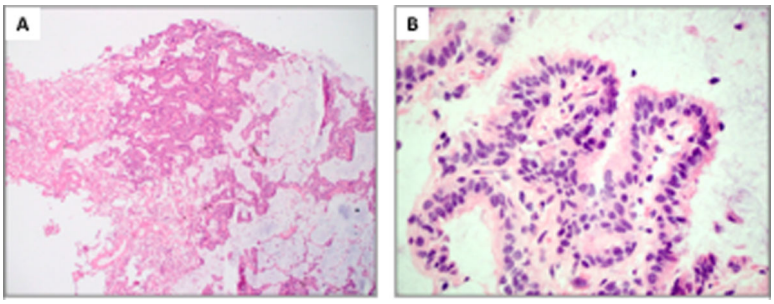

Figure 6.

Frozen section of bronchiolar adenomas. A, Low power shows abundant intra-alveolar mucin and seemingly discontinuous growth, raising the differential diagnosis of IMA (Patient 5, case 2). B, Apical cilia often appear as indistinct, ruffled borders and can be nearly impossible to visualize, even at high magnification (Patient 8, case 1).

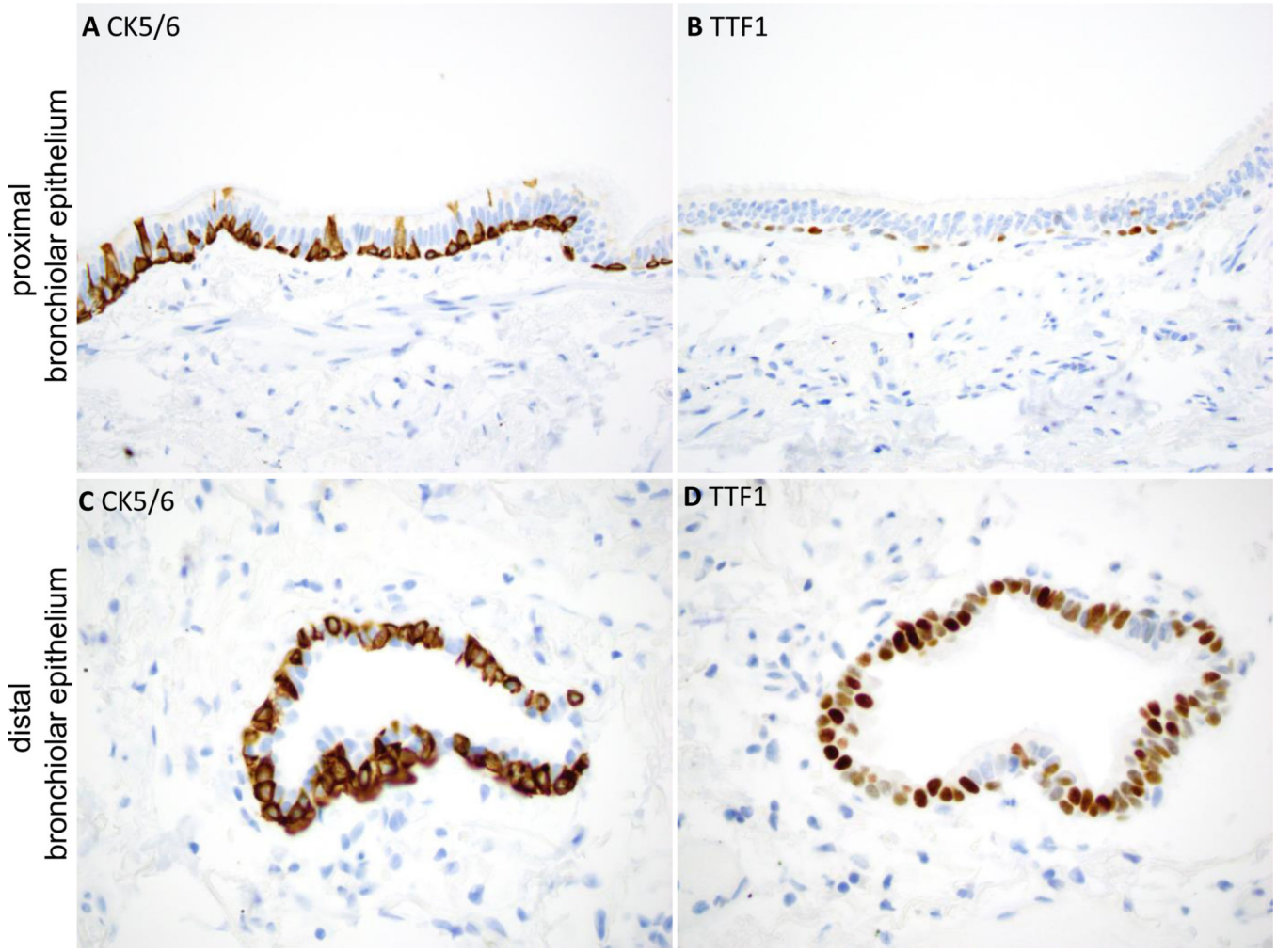

Figure 7.

Immunophenotype of normal proximal and distal bronchiolar epithelium.

In proximal bronchiolar epithelium (A and B), the luminal cells are largely negative for TTF1. The basal cells show strong positivity for CK5/6 (or p40) and weak focal positivity for TTF1.

In distal bronchiolar epithelium (C and D), the luminal cells show stronger and more diffuse positivity for TTF1. The basal cells show strong positivity for CK5/6 (or p40), and patchy weak to moderate positivity for TTF1.

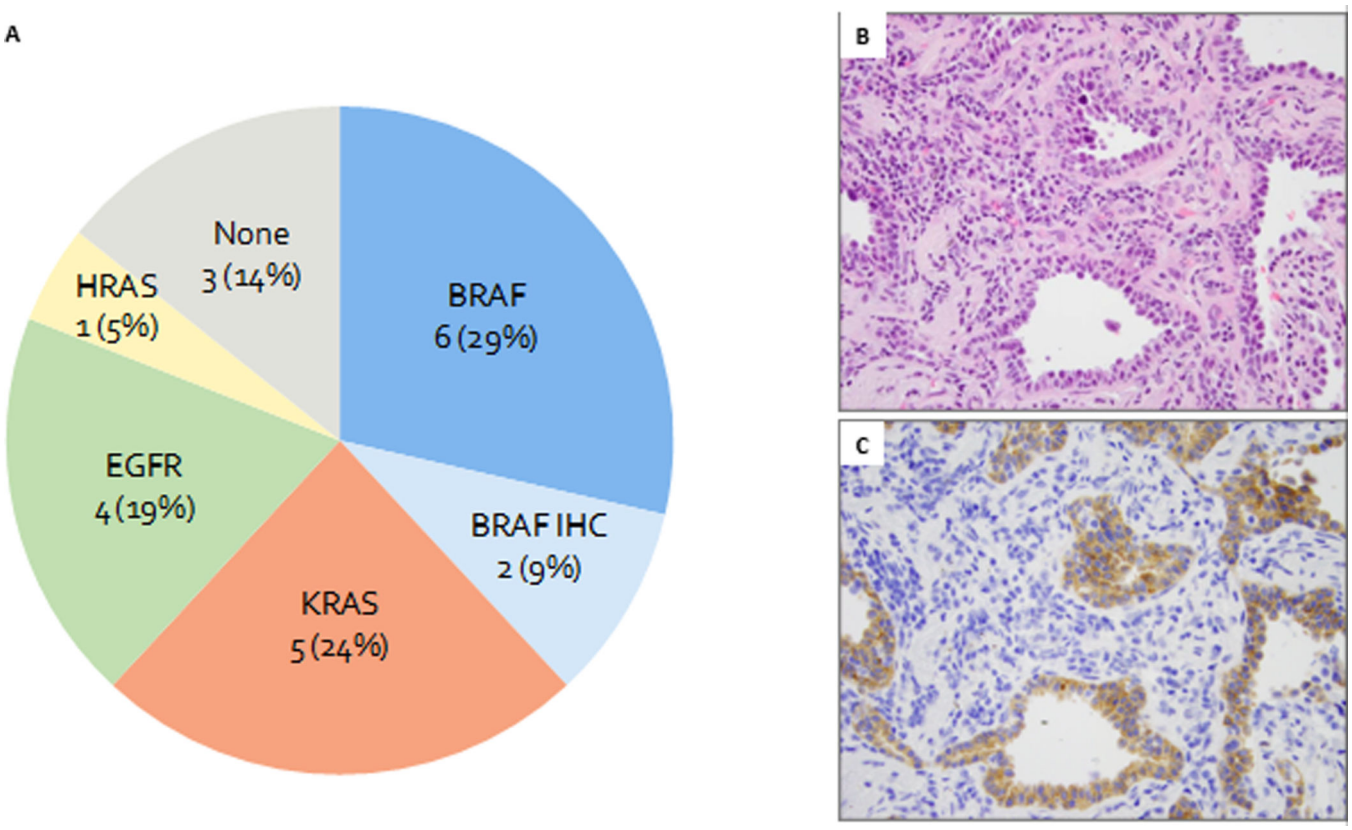

Figure 8.

Molecular finding in bronchiolar adenomas.

A. Results of molecular studies and BRAF immunohistochemistry on 21 bronchiolar adenomas.

B. H&E of a *BRAF* V600E mutant bronchiolar adenoma (Patient 8, case 2).

C. BRAF V600E staining shows cytoplasmic positivity in both luminal and apical cells.

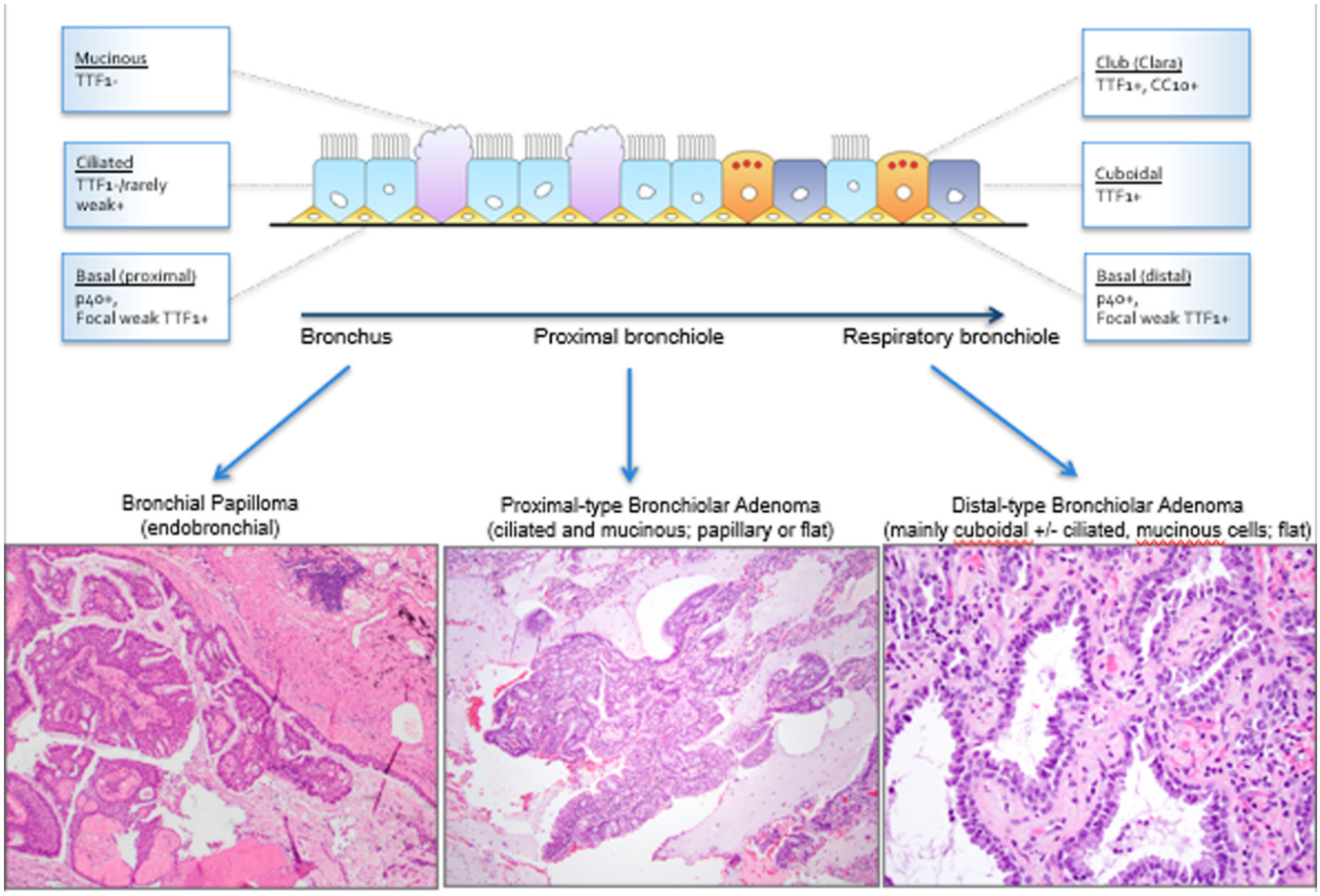

Figure 9.

Diagram summarizing the relationship between the spectrum of differentiation in normal bronchioles and bronchiolar adenomas.

Table 1

Clinicopathologic features of 25 bronchiolar adenomas from 21 patients

Patient-Tumor	Age	Sex	Smoking History	Size (cm)	Morphology	Architecture	Mucinous Cells	Cilia	Discontinuous Spread	Frozen Section Diagnosis	Original Diagnosis	TTF1 in luminal cells	TTF1 in basal cells*
1	75	M	Yes	0.3	Proximal	Papillary	Present	Present	Absent		CMPT	Weak/focal	Patchy
2	78	M	No	2.0	Proximal	Papillary	Present	Present	Absent	CMPT	CMPT	Negative	Weak/focal
3	73	F	Yes	0.9	Proximal	Papillary	Present	Present	Present	IMA	Glandular papilloma	Negative	Negative
4	68	M	No	1.0	Proximal	Papillary	Present	Present	Present		Glandular papilloma	Negative	Negative
5	77	F	N/A	1.4	Proximal	Flat	Present	Present	Absent		AIS	Negative	Weak/focal
6	73	M	Yes	1.2	Proximal	Flat/papillary	Present	Present	Absent		CMPT	Negative	Weak/focal
7	69	M	Yes	0.3	Proximal	Flat/papillary	Present	Present	Absent		CMPT	ND	ND
8–1	83	F	Yes	0.6	Proximal	Flat/papillary	Present	Present	Present	ADCA	CMPT	Weak/focal	Weak/focal
8–2	83	F	Yes	0.7	Distal	Flat	Absent	Absent	Absent	ADCA	AIS	Positive	Positive
8–3				0.2	Distal	Flat	Absent	Absent	Absent		AAH	ND	ND
9–1	76	F	Yes	0.5	Distal	Flat	Focal	Focal	Absent		CMPT	Positive	Positive
9–2				0.5	Distal	Flat	Rare	Rare	Absent		Basal cell hyperplasia	Positive	Positive
10–1	77	M	Yes	0.25	Distal	Flat	Focal	Present	Present		CMPT	Positive	Positive
10–2				0.25	Distal	Flat	Absent	Absent	Absent		CMPT	Positive	Positive
11	78	F	Yes	0.3	Distal	Flat	Focal	Focal	Absent		CMPT	Positive	Positive
12	69	M	Yes	0.2	Distal	Flat	Rare	Present	Absent		PBM	Positive	Positive
13	74	M	Yes	0.5	Distal	Flat	Present	Focal	Absent	MGA	CMPT	ND	ND
14	55	F	No	0.5	Distal	Flat	Absent	Present	Absent		PBM	Positive	Positive
15	66	M	No	1.9	Distal	Flat/papillary	Absent	Absent	Absent		AIS	Positive	Positive
16	68	F	Yes	0.4	Distal	Flat/papillary	Focal	Absent	Present		CMPT	Positive	Positive
17	78	M	Yes	1.5	Distal	Flat	Present	Focal	Present		CMPT	Positive	Positive
18	56	F	N/A	1.2	Distal	Flat	Focal	Focal	Present	ADCA	CMPT	Positive	Positive
19	72	F	Yes	0.5	Distal	Flat/papillary	Focal	Present	Present	ADCA	CMPT	ND	ND
20	68	F	Yes	0.2	Distal	Flat/papillary	Focal	Present	Present	ADCA	CMPT	Positive	Positive

Am J Surg Pathol. Author manuscript; available in PMC 2021 April 23.

Patient-Tumor	Age	Sex	Smoking History	Size (cm)	Morphology	Architecture	Mucinous Cells	Cilia	Discontinuous Spread	Frozen Section Diagnosis	Original Diagnosis	TTF1 in luminal cells	TTF1 in basal cells*
21	61	M	N/A	1.2	Distal	Flat	Focal	Present	Absent	ADCA	Glandular papilloma	ND	ND

AAH: atypical adenomatous hyperplasia; AIS: adenocarcinoma in situ; ADCA: adenocarcinoma; CMPT: ciliated muconodular papillary tumor; IMA: invasive mucinous adenocarcinoma; MGA: mucous gland adenoma; PBM: peribronchiolar metaplasia

*p40 and CK5/6 show diffuse and strong labeling in basal cells in all cases

Table 2

Genomic alterations of 25 bronchiolar adenomas from 21 patients

Patient-Tumor	Morphology	Methodology	Number of genes tested	Putative Driver Mutation	Secondary Mutations	BRAF IHC	Driver in concurrent adenocarcinoma
1	Proximal	Ampliseq	98	*BRAF* p.V600E (COSM476)		Positive	*KRAS* p.G12C
2	Proximal	ARMS	9	Not detected		ND	
3	Proximal	Ampliseq	98	Not detected		Negative	
4	Proximal	Ampliseq	98	Not detected		Negative	
5	Proximal	Ampliseq	98	*EGFR* ex20 p.D773_N774insNPH (COSM12381) *		Negative	
6	Proximal	Ampliseq	98	*KRAS* p.G12D (COSM521)		Negative	
7	Proximal	Ampliseq	50	*KRAS* p.G12V (COSM520)		Negative	
8–1	Proximal	Ampliseq	98	*EGFR* ex19 p.E746_S752>V (COSM12384)		Negative	
8–2	Distal	Ampliseq	98	*BRAF* p.V600E (COSM476)		Positive	
8–3	Distal	Ampliseq	N/A	Failed (low tumor)		Negative	
9–1	Distal	MSK-IMPACT	410	*BRAF* p.V600E (COSM476)		Positive	*KRAS* p.G12C
9–2	Distal	MSK-IMPACT	410	*BRAF* p.V600E (COSM476)		Positive	
10–1	Distal	Ampliseq	98	*HRAS* p.G13R (COSM486)	*BRAF* p.G464V (COSM450)	Negative	
10–2	Distal	Ampliseq	98	*BRAF* p.V600E (COSM476)		Positive	
11	Distal	MSK-IMPACT	410	*BRAF* p.V600E (COSM476)		Positive	*KRAS* p.G12D
12	Distal	IHC only	N/A	*BRAF* p.V600E (COSM476)		Positive	*EGFR* p.E746_A750del
13	Distal	IHC only	N/A	*BRAF* p.V600E (COSM476)		Positive	
14	Distal	Ampliseq	98	*EGFR* ex20 p.D773_N774insNPH (COSM12381) *		Negative	
15	Distal	Ampliseq	6	*EGFR* ex19 p.L747_S752del (COSM6255)	*EGFR* ex19 p.D761Y (COSM21984)	ND	
16	Distal	Ampliseq	98	*KRAS* p.G12C (COSM516)	*U2AF1* p.S34F (COSM166866)	Negative	*KRAS* p.G12A
17	Distal	Ampliseq	98	*KRAS* p.G12V (COSM520)	*U2AF1* p.S34F (COSM166866)	Negative	
18	Distal	Ampliseq	98	*KRAS* p.G12D (COSM521)	*U2AF1* p.S34F (COSM166866)	Negative	
19	Distal	MSK-IMPACT	N/A	Failed (low tumor)		ND	

Patient-Tumor	Morphology	Methodology	Number of genes tested	Putative Driver Mutation	Secondary Mutations	BRAF IHC	Driver in concurrent adenocarcinoma
20	Distal	ND	N/A	ND		Negative	
21	Distal	ND	N/A	ND		Negative	

* Alternative annotation: N771_H773dup

Table 3

Comparison table of proximal- and distal-type bronchiolar adenomas

	Proximal-type BA	**Distal-type BA**
Cases/Patients	8/8	17/14
Median age (range)	76 (68–83)	71 (55–83)
M:F	5:3	6:8
Ethnicity	2 Asian 4 Caucasian 2 Not specified	9 Caucasian 5 Not specified
Median tumor size (range)	1.0 cm (0.3 – 2.0 cm)	0.5 cm (0.2 – 1.9 cm)
Driver mutations BRAF EGFR KRAS HRAS	 1 (12%) 2 (25%) 2 (25%) 0	Out of 13 with molecular: 7 (54%) 2 (15%) 3 (23%) 1 (8%)
Total with driver	5 (62%)	13 (100%)

Am J Surg Pathol. Author manuscript; available in PMC 2021 April 23.